◇ Monograph Excerpt ◇

Matter Antimatter Fluctuations

search, discovery and analysis of Bs flavor oscillations

Nuno Leonardo

Complete work published as:
Analysis of B_s oscillations at CDF, MIT Thesis (2006)
Matter antimatter fluctuations, Monograph, LAP Lambert (2011)

Chapter 6

Flavor tagging

The flavor of B mesons refers throughout this monograph to their particle B or anti-particle $\bar{B}$ state. It is, equivalently, given by the corresponding $\bar{b}$ or b quark content: a meson state B_q, where q denotes a u, d or s quark, contains a $\bar{b}$ quark; a $\bar{B}_q$ state is formed instead of a b quark. The B meson candidates are reconstructed in flavor specific final states, listed in Table 4.1. For example, in $B \to D\pi$ and $B \to DlX$ decays, the positively (negatively) charged pion or lepton is associated to a B ($\bar{B}$) state. The flavor at decay time is therefore determined from the decay products of the B meson candidate. For neutral B meson systems, B^0 or B_s, mixing occurs between the two flavor states, B-$\bar{B}$, as these do not coincide with the corresponding mass eigenstates (Section 2.1). The study of flavor oscillations which occur in these systems therefore requires, in addition to the determination of the final state meson flavor, the identification of the B-flavor at production time. Several flavor tagging techniques are used in this task.

In the Tevatron's $p\bar{p}$ collisions b-hadrons are produced from the hadronization of b-quarks originating from $b\bar{b}$ pairs produced in the hard parton interactions. The B meson whose decay products satisfy the trigger requirements is referred to as the "trigger B", while the other b-hadron in the event is called the "opposite-side B". The flavor tagging algorithms may also be broken down into two classes: *same-side tagging* (SST) and *opposite-side tagging* (OST). The former explores flavor-charge correlations between the trigger B and tracks nearby in phase space, while the latter is based on the identification of some property of the opposite-side B to determine its b quantum number, from which the production flavor of the trigger B can be inferred.

A distinguishing aspect between the same-side and opposite-side methods is that the performance of the former depends on the species of the B meson candidate being tagged, while that of the latter does not. This is the case as the hadronization of the b quark and of the $\bar{b}$ quark take place in an incoherent fashion. It follows, in particular, that the properties

of the OST algorithms may be measured for instance in samples of B^+ and B^0 mesons and transferred directly to samples of B_s mesons. This possibility is also explored in the coming chapters. The same strategy is not applicable in the case of the SST method.

The SST and OST techniques are explored respectively within and outside an isolation domain which, for a given event, corresponds to a cone ΔR of 0.7 around the reconstructed B candidate direction. The two classes of tagging algorithms make in this way use of uncorrelated information.

In general, for realistic algorithms and depending also on the characteristics of each event, a flavor tagging method does not always give a correct answer and sometimes fails alltogether to make a decision. Let, for a given sample, N_r denote the number of candidates correctly tagged, N_w denote the number of incorrect tags, and N_n the number of candidates for which the tagger failed to provide a decision. The following quantities are thus conveniently defined. The tagging *efficiency*, ϵ, is given by the fraction of events which are non-trivially tagged, that is for which the algorithm provides a definite decision,

$$\epsilon \;=\; \frac{N_r + N_w}{N_r + N_w + N_n}\,. \tag{6.1}$$

The tagging *dilution*, $\mathcal{D}$, is a measure of the quality of the tagging decision,

$$\mathcal{D} \;=\; \frac{N_r - N_w}{N_r + N_w}\,, \tag{6.2}$$

being related to the mistagging probability, $w = N_w/(N_r + N_w)$, by $\mathcal{D} = 1 - 2w$.

The tagging *effectiveness*, $\epsilon\mathcal{D}^2$, provides the figure of merit of a tagging algorithm. It effectively scales the size of a mixing sample: the statistical power of a sample of size N tagged by the algorithm is equivalent to that of a perfectly tagged sample of size $N\,\epsilon\mathcal{D}^2$. Accordingly, the expected statistical uncertainty, σ, in a mixing measurement becomes (11.17)

$$\sigma \;\propto\; \frac{1}{\sqrt{N \cdot \epsilon\mathcal{D}^2}}\,. \tag{6.3}$$

In developing and optimizing a tagging algorithm it is therefore the tagging power $\epsilon\mathcal{D}^2$, rather than ϵ and $\mathcal{D}$ separately, which is to be maximized.

6.1 Opposite side tagging

A highest quality opposite-side tagging method would involve the full reconstruction of the opposite-side B, and discovering it to be, say, a charged B meson which does not undergo flavor mixing. From this one would be assured of the b or $\bar{b}$ quark content of the opposite-side B, and thus also of the production flavor of the trigger B which would be the opposite.

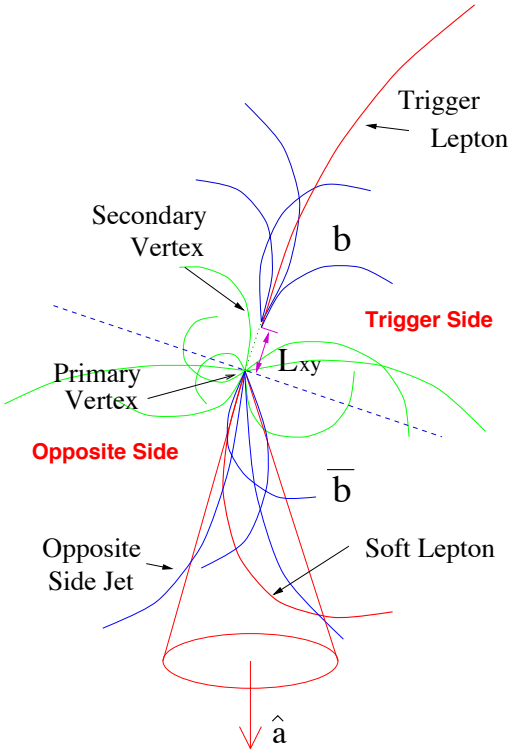

Figure 6.1: Illustration of a $b\bar{b}$ event and opposite-side tagging.

Although the dilution would be maximal (*i.e.* unity) for such an algorithm, in practice the efficiency for reconstructing completely the opposite-side b hadron is much too small to be useful. Instead of the full reconstruction, thus, inclusive properties of the opposite-side B indicative of its flavor are employed, this way achieving an appropriate compromise between dilution and efficiency.

The tagging methods specifically explore the sign of the charge of leptons originating from semileptonic decays of the opposite-side B, as well as that of the opposite-side b-jets.

The performance of the algorithms is established in a high statistics inclusive B semileptonic trigger sample. The trigger and opposite sides are illustrated in Figure 6.1. These will be further described below. The performance is ascertained by comparing the charge of the trigger side lepton with that of the opposite-side lepton or jet. Each event is classified accordingly into one of the following three mutually exclusive categories: the charge of the trigger lepton coincides with (i) or is opposite to (ii) the charge of the opposite-side lepton or jet, or, otherwise, (iii) the latter cannot be inferred for the event. The number of events in each class is used as an estimate of the number of incorrectly tagged (N_w), correctly tagged (N_r), and non-tagged (N_n) events, respectively. These estimates are in turn used to compute

the efficiency (6.1) and dilution (6.2) of the algorithm, after having taken into account effects having to do with the sample composition and mixing.

6.1.1 Soft lepton taggers

Lepton tagging exploits the charge sign of the lepton in the decays $b \to Xl$. In case the lepton originates from the semileptonic decay of the opposite-side B,

$$b \to c\, l^- \bar{\nu}_l X\,, \qquad \bar{b} \to \bar{c}\, l^+ \nu_l X\,,$$

and in case the latter did not undergo flavor oscillation, the lepton charge determines the production b-flavor.

The accuracy of this determination is affected in principle by several factors. In an ensemble of tags, the opposite-side b hadron can be seen as a mixture of B^+, B^0, B_s and other meson and baryon states, which are not identified. While the B^+ and b baryons fully contribute, the neutral B mesons however undergo flavor mixing: a fraction of the B^0 mesons will have oscillated into a state different from the production state before decaying, thus giving an incorrect tag, and the B_s system, being fully mixed, does not provide any tagging power. It may happen, additionally, that the lepton does not come from the direct b semileptonic decay, but instead from the sequential transition $b \to c \to lX$. The charge of the lepton is in this case opposite to that of the direct decay, and results in an incorrect tag. It may also happen that the lepton candidate is misidentified, *i.e.* that it is fake. The overall correctness of the flavor determination is statistically determined, and expressed by the tagging dilution.

The method is explored and optimized for muon and electron samples and the corresponding algorithms are respectively named *soft muon tagger* (SMT) [56] and *soft electron tagger* (SET) [57]. In each case, a multivariate lepton likelihood $\mathcal{L}^l$ ($l = \mu, e$) is constructed for discriminating real from fake leptons. It combines information from the various calorimeter and muon detector subsystems, along with track matching and additional lepton identification variables. The lepton likelihood estimator is constructed as

$$\mathcal{L}^l \;=\; \frac{S^l}{S^l + B^l} \tag{6.4}$$

where the signal S^l and background B^l likelihood terms

$$S^l = \prod_i S_i^l\,, \qquad B^l = \prod_i B_i^l\,, \tag{6.5}$$

are given as the product of the corresponding probability distributions of the employed discriminating variables. The set of used variables is specific to each algorithm, and is given

below. The likelihood construction (6.4) implies that it is expected to approach unity for real leptons and zero for fake leptons.

Dependences of the methods' dilutions are further explored, in terms of the lepton likelihood, the transverse momentum of the lepton relative to the axis of the jet to which it belongs, and, for muon candidates, the involved muon detector subsystems.

Muon identification

Muons are identified as charged particles which traverse the tracking and calorimeter systems of the detector, reaching the muons chambers. A muon candidate thus consists of a stub in a muon chamber associated with a COT track that extrapolates in the vicinity of the stub. The matching between the muon stub and the extrapolated track is quantified through the variables ΔX, $\Delta\Phi$, and ΔZ. These matching variables depend on the muon transverse momentum. For muons of lower momenta the effects of multiple scattering are larger, and the matching is less accurate. Momentum independent matching variables are obtained after rescaling with the corresponding p_T dependent widths, $\Delta x = \Delta X/\sigma_{\Delta X}$, $\Delta\phi = \Delta\Phi/\sigma_{\Delta\Phi}$, and $\Delta z = \Delta Z/\sigma_{\Delta Z}$.

In addition to the track–stub matching variables, the energy depositions by the muon candidate in the electromagnetic and hadronic calorimeters, denoted $E_{\rm em}$ and $E_{\rm had}$, are considered as well. Dependences of $E_{\rm had}$ on the transverse momentum of the muon candidate are considered, by parameterizing it in three p_T ranges. Momentum dependences are neglected for $E_{\rm em}$. The isolation, I, of a track j is defined as the ratio between the track transverse momentum, p_T^j, and the sum of the transverse momenta of all tracks within a cone $\Delta R < 0.4$ about the track j,

$$I \;=\; \frac{p_T^j}{\sum_i p_T^i}\,, \qquad \Delta R(i,j) = \sqrt{\Delta\eta^2 + \Delta\phi^2} < 0.4\,. \tag{6.6}$$

To account for the dependence of the electromagnetic energy distribution on isolation, different $E_{\rm em}$ templates are used for isolated ($I > 0.5$) and non-isolated ($I < 0.5$) muons. No noticeable dependence on isolation is observed for $E_{\rm had}$.

The characteristic behavior of the discriminating variables for real muons is extracted from samples of $J/\psi \to \mu^+\mu^-$ decays. Fake muon candidates may be produced by misidentified pions, kaons, and protons that reach the muon chambers by punching-through the calorimeters. These are studied in samples of $K^0_s \to \pi^+\pi^-$ (pions), $D^0 \to K^-\pi^+$ (kaons) and $\Lambda^0 \to p^+\pi^-$ (protons) decays. The obtained distributions of the discriminating variables – Δx, $\Delta\phi$, Δz, $E_{\rm em}$, $E_{\rm had}$ – for both real and fake muons are taken as templates for forming the likelihood factors S^μ and B^μ according to (6.5). The most discriminating power is provided

by the hadronic energy distributions, and, especially for high p_T muon candidates, by the track-stub matching quantities.

Electron identification

Electrons are identified as charged particles whose energy is deposited mostly in the electromagnetic calorimeter. Electron candidates consist of COT tracks that extrapolate to the calorimeter, satisfying the thresholds of 1.0 GeV/c in transverse momentum and of 0.8 GeV/c^2 in transverse electromagnetic energy. A 2-tower cluster is formed by adding to the extrapolated seed tower its nearest neighboring tower in z if the transverse energy deposited therein exceeds 100 MeV/c^2. The electromagnetic energy $E_{\rm em}$ is defined as the combined deposited energy in the 2-tower. The hadronic energy $E_{\rm had}$ is evaluated in a similar fashion. The local isolation I of a track is defined, similarly to (6.6), as the ratio of its transverse momentum to the sum of transverse momenta of the tracks in a $\Delta R < 0.7$ cone which extrapolate to the 2-tower cluster. Locally isolated candidates ($I = 1$) are required to satisfy $E_{\rm had}/E_{\rm em} < 0.125$, while for locally non-isolated candidates ($I < 1$) $E_{\rm had}/E_{\rm em} < 0.5$ is imposed. The ratio of the electromagnetic energy to the track momentum, $E_{\rm em}/p$, is a strong discriminator against pions particularly for isolated electron candidates.

Further discriminating information is provided by the maximum shower (CES) and the central pre-radiator (CPR) detector sub-systems. The χ^2 matching variables in the CES, χ^2_x and χ^2_z, provide a comparison of the shower profiles in the CES wire and strip views with the same profiles extracted from electron test beams. The variable $E_{\rm ces}/p^*$ corresponds to the corrected wire cluster pulse height in the CES, and provides very good separation between electrons and pions even at low p_T. The CES variables ΔX and ΔZ correspond to the distance in the transverse and r-Z planes, between the track extrapolated to the CES radius and the actual cluster position measured in the CES. These are stabilized against p_T variations by scaling with the corresponding p_T dependent widths, $\Delta x = \Delta X/\sigma_{\Delta X}$ and $\Delta z = \Delta Z/\sigma_{\Delta Z}$. Δx is further signed with the track charge. Distributions of these variables are formed for locally isolated and non-isolated candidates, and their discriminating power increases with p_T. The pulse height in the CPR corrected for its $\sin(\theta)$ dependence, $Q_{\rm cpr}$, is a rather strong discriminator between electrons and pions. The same is also true for the energy loss measured in the COT, dE/dx, whose usefulness is enhanced by the fact that, unlike the CES and CPR based variables, its separation power increases with the p_T of the track candidate.

A pure electron sample is obtained by reconstructing electrons from photon pair-conversions, $\gamma \to e^+e^-$. Hadrons such as pions, kaons, and protons can also fake electron candidates. Properties of fake candidates are obtained from samples of $K^0_s \to \pi^+\pi^-$ decays. These

samples are used to extract parameterized distributions of the discriminating variables – $E_{\rm had}/E_{\rm em}$, $E_{\rm em}/p$, χ^2_x , χ^2_z , $q\Delta x/\sigma_x$, $\Delta z/\sigma_z$, $E_{\rm ces}/p^*$, $Q_{\rm cpr}$, dE/dx – for both real and fake electrons, to form the associated likelihood factors S^e and B^e as in (6.5).

Tag selection

When the algorithms are employed to tag the production flavor of a B meson candidate, certain criteria are applied to the potential soft lepton candidates and, if those criteria are satisfied, one of them is finally elected to provide the tag decision.

The soft lepton candidates are required not to coincide with the reconstructed daughter tracks of the trigger-side B meson. The transverse momentum is required to exceed 1.5 GeV/c and 2.0 GeV/c for muon and electron candidates, respectively. An impact parameter requirement of $|d_0| < 0.3$ cm is used to help rejecting hadrons which decay into muons. Track quality requirements of at least 10 axial and 10 stereo COT hits along with at least 2 SVX r-ϕ hits are imposed on electron candidates.

Jets present in the event are found based on a track cone clustering algorithm [76]. If multiple candidates satisfy the mentioned criteria, a globally isolated lepton (no other tracks found within $\Delta R = 0.7$) is chosen if found. Otherwise, the appointed candidate is that with the highest relative transverse momentum p_T^{rel} with respected to the jet axis to which it belongs.

Few additional criteria are further imposed bearing in mind the concurrent application of the various tagging methods to common mixing samples. A minimum lepton likelihood of 0.05 is required for both electron and muon candidates; events with such poor quality soft leptons are expected to be more accurately tagged with the jet charge method.

Dilution dependences

The performance of the tagging algorithms shows expected dependences that are explored. Namely, once quantities on which the performance depends are identified, rather than imposing hard thresholds for selecting only the best quality tags, the dilution is instead parameterized in terms of such variables. The tagging efficiency is not decreased, and the more reliable tag gets a higher weight thus enhancing the overall tagging power.

One such variable is the lepton likelihood, $\mathcal{L}^l$. The dilution increase with increasing values of the lepton likelihood is accounted for, and shown in Figure 6.2. This behavior is expected based on that a more pure lepton sample should reflect the b flavor more accurately.

The dilution is verified also to increase with the transverse momentum p_T^{rel} of the lepton with respect to the axis of the jet in which the lepton is found. An adequate empirical

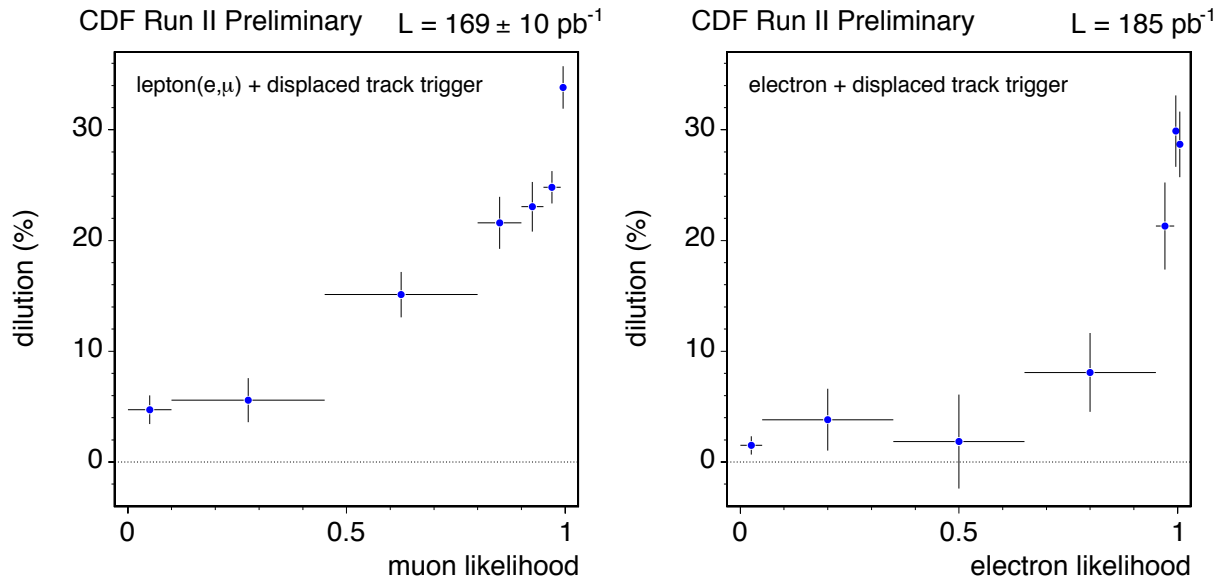

Figure 6.2: Dilution dependencies of the soft lepton taggers as a function of the muon and electron likelihoods; the various muon types have been combined on the left plot.

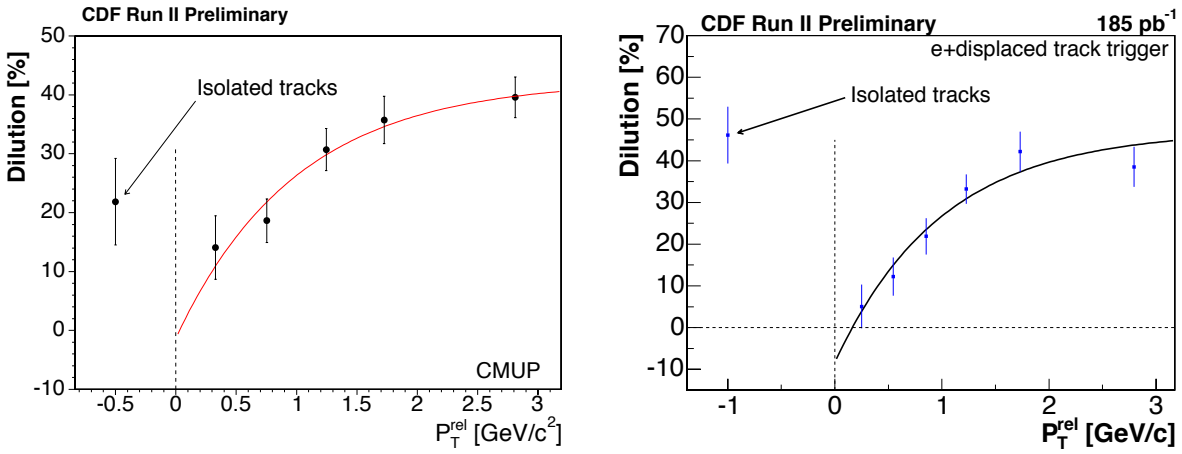

Figure 6.3: Dilution dependencies of the soft lepton taggers as function of the transverse momentum relative to the jet axis: (left) SMT for CMUP muon type, (right) SET for $\mathcal{L}^e > 0.85$.

description of this dependence is provided by

$$\mathcal{D}(p_T^{rel}) \;=\; A_\ell \left(1 - e^{-p_T^{rel}+\delta_\ell}\right) \,. \tag{6.7}$$

and is shown in Figure 6.3. This qualitative behavior originates from the fact that leptons coming from b quark decays tend to be more widely spread in the plane transverse to the b direction than in jets originating from lighter quarks, due to the larger phase space available.

For the SMT algorithm, a separate implementation is derived according to the detector sub-system which identifies the muon stub: CMU, CMP, CMUP (muons with stubs in both CMU and CMP), CMX, and IMU.

6.1.2 Jet charge taggers

Jet charge tagging exploits the charge of jets on the opposite-side. If the jet which originates from the opposite-side b-quark is identified, the charge sign of the b, and thus its flavor, is expected to be given on average by the sign of the weighted sum of the charges of tracks forming the jet.

The implementation [77] of the method takes as input various track and jet properties. The way the various discriminating quantities are extracted and characterized, as well as combined, is distinct from the strategy employed in the case of the SLTs described in Section 6.1.1. Samples of Monte Carlo events are used to study $b\bar{b}$ properties. Good agreement needs thus to be achieved between the relevant quantities extracted from these samples and those observed in the data, which is accomplished by taking into account in the simulation additional $b\bar{b}$ pair creation processes beyond the leading order $b\bar{b}$ production mechanism. The b-jet properties are extracted from these samples which are finally used for jet selection in the data. The available quantities are then combined in an artificial neural network (NN). An improved combination relative to that which could be obtained via a likelihood ratio is achieved, as correlations between the various input quantities are intrinsically taken into account.

Probabilities that individual tracks belong to B decay products are estimated; these are used to define jet variables, which are combined to provide b-jet probabilities. Once the highest probability jet is selected, the flavor decision provided by the method is given by the sign of the charge computed for the tagging jet as

$$Q_{\rm jet} \;\equiv\; \frac{\sum_i q^i\, p_T^i\, (1 + T_P^i)}{\sum_i p_T^i\, (1 + T_P^i)} \tag{6.8}$$

where the index i runs over all tracks in the jet, q^i is the charge of the i-th track, p_T^i its transverse momentum, and T_P^i is the track probability indicating how likely it is to be a b daughter. The method is optimized for three mutually exclusive categories of jet quality:

Class 1 (JVX): jets containing an identified secondary vertex, with decay length significance $L_{xy}/\sigma_{L_{xy}}$ greater than 3,

Class 2 (JJP): jets not in the above class and with at least one track with probability T_P greater then 50%,

Class 3 (JPT): jets not in the above classes.

These classes provide different tagging performances and are characterized separately. Dilution dependencies on the jet charge $Q_{\rm jet}$ and NN output for jet probability are further explored and parameterized.

Jet reconstruction

All opposite-side tracks are first identified. These are defined, for each event, to be those found outside the isolation cone $\Delta R > 0.7$ relative to the momentum direction of the trigger B, with tracks used in its reconstruction being explicitly excluded. Tracks need then to satisfy requirements on impact parameter ($|d_0| < 0.15$ cm), on z_0 ($|z_0 - z_B| < 1$ cm), and on transverse momentum ($p_T > 0.4$ GeV/c) to be considered as candidate jet constituents.

Jets in an event are found using a standard CDF software package [76] which implements a track based cone clustering algorithm. Those tracks with $p_T > 1.0$ GeV/c are considered as jet seeds. Pairs of such tracks within a cone ΔR of 1.5 are merged, thus forming new seeds with momentum given by the sum of the momenta of the two original tracks. The procedure is repeated until no track pairs satisfy the merging criteria. Finally, jets are formed by adding to these final seeds the remaining, lower p_T tracks within a cone ΔR of 1.5.

Track probability

Tracks are assigned probabilities for having originated from a B decay chain. This is achieved with a neural network, which is optimized on Monte Carlo events. The NN output is evaluated during the learning process on the basis of track matching to the generator level information.

The input quantities to the NN are selected based on the power to discriminate between whether the track was created at the primary or a secondary vertex, in conjunction with the corresponding level of agreement between data and Monte Carlo. Among the most powerful input variables are the track impact parameter d_0, along with its impact parameter significance δ_0/σ_{d_0} signed with respect to the jet momentum $\vec{p}_{\rm jet}$, with

$$\delta_0 = |d_0| \, \mathrm{sign}(\vec{d_0} \cdot \vec{p}_{\rm jet}) \, .$$

The transverse momenta and ΔR, along with the track rapidity with respect to the jet axis are also provided.

The structure employed for the track probability NN consists of three neuron layers. Each input variable is associated to one node in the input layer, the intermediate layer contains six nodes, and the output layer if formed of a single node which provides the network decisions.

Jet probability

The jets reconstructed on the opposite side may have varying characteristics, depending on several factors, which for instance include the presence of the opposite-side B in the detector acceptance, its momentum and decay length. Probabilities are assigned for the candidate jets which indicate the likelihood for being a b-jet. This is achieved employing a neural network combining several jet variables; a three layer structure similar to that used for the track NN is chosen. Several of these variables are constructed using the track probability, denoted T_P, information previously obtained. The weighted number of tracks in the jet is given by $\sum_i T_P^i$. The jet probability J_P is computed as

$$J_P \;=\; P_N \sum_{j=0}^{N-1} \frac{(-\ln P_N)^j}{j!} \qquad \text{with} \quad P_N = \prod_{i=1}^{N} T_P^i \,.$$

Input variables related to properties of secondary vertices, such as the corresponding χ^2 probability, the momentum fraction and the number of tracks involved are considered. Other variables are related to the kinematics and the shape of the jet, such as p_T, invariant mass, and jet spread.

Dilution dependences

Once the tagging jet is identified as the highest probability jet, the method's decision is provided by the sign of the effective charge of the jet in (6.8).

The correctness of this decision is reflected in the tagging dilution. The latter is observed to depend on the following two independent variables: the absolute value of the jet charge $|Q_{\text{jet}}|$, as computed in (6.8), and the jet probability variable P_{nn}, returned by the b-jet probability NN. The dilution increases with the two variables as expected, and its dependency is observed to be linear. In order to take advantage of such dependencies, each of the samples of tagging jet classes – JVX, JJP, and JPT – is further divided in 10 bins of the variable $|Q_{\text{jet}}| \cdot P_{\text{nn}}$, along with an extra bin for jets containing a single track. These dependencies are illustrated in Figure 6.4.

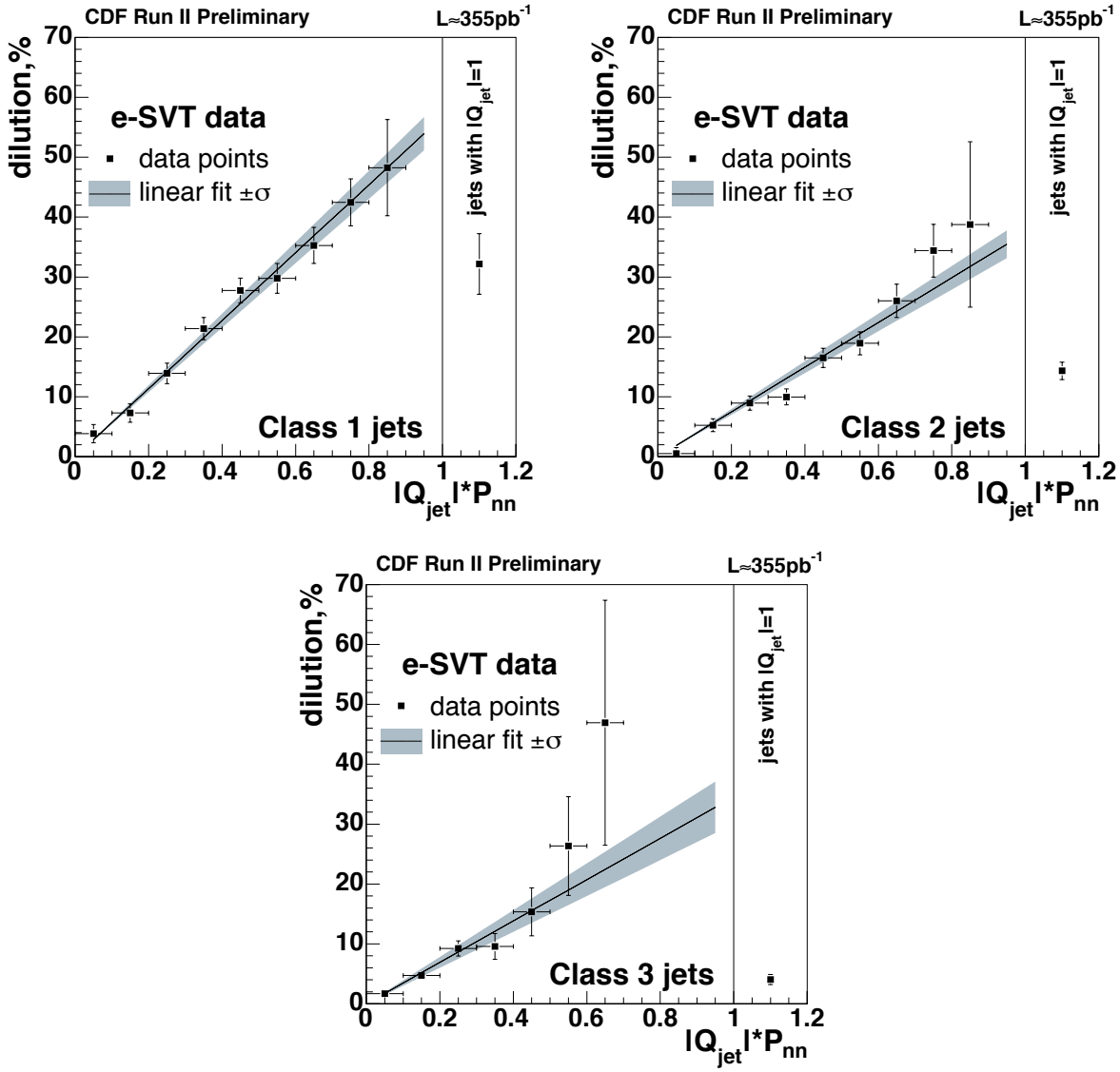

Figure 6.4: Dilution dependency on $|Q_{\rm jet}| \cdot P_{\rm nn}$, for each of the jet charge classes: (1) JVX, (2) JJP and (3) JPT.

6.1.3 Tagging performance

Data sample

The opposite-side tagging algorithms are established in an inclusive sample rich in B mesons, collected with the *lepton and displaced track trigger* described in Section 4.1. The large sample size allows for the exploration of dilution dependencies and reasonably accurate parameterizations in terms of relevant characteristics of the events. The sample sizes used for the soft lepton and jet charge taggers correspond to integrated luminosities of approximately 180 and 355 pb^{-1}, respectively.

The employed trigger sample is a not a pure sample of B decays. In addition to events from semileptonic B decays it also contains semileptonic charm decays, hadrons that fake the trigger lepton, and other backgrounds. Several of these background contributions are removed by imposing an event selection criteria which restrict the invariant mass of the lepton and displaced track system to the range of $(2.0, 4.0)$ $\mathrm{GeV/c^2}$. To remove the effect of remaining background events, a subtraction procedure is applied to the distributions of interest. The procedure is based on the assumption that the background sources are symmetric in the signed impact parameter of the displaced track defined as

$$\delta_0^{\mathrm{SVT}} \equiv |d_0| \,\mathrm{sign}(\vec{d_0} \cdot \vec{p}_{l,\mathrm{SVT}}) \,,$$

where $\vec{d_0}$ points from the primary vertex to the point of closest approach of the displaced track, and $\vec{p}_{l,\mathrm{SVT}}$ is the the combined momentum of the trigger lepton and the displaced track. Figure 6.5 shows the mass distributions of the lepton and displaced track pair for positive and negative signed impact parameter δ_0^{SVT}. Distributions characteristic of pure signal events are obtained by subtracting the distribution with negative δ_0^{SVT} from the corresponding distribution with positive signed impact parameter [78]. In particular, this subtraction procedure is applied in the determination of the number of signal events belonging to each of the tagging classes used in the computation of the two quantities of interest: the efficiency and the dilution of the tagging algorithms.

Given that the trigger-side B meson is only inclusively reconstructed, a few additional track selection requirements are imposed for reinforcing that no trigger-side B daughters are considered as tag candidates. Both the trigger lepton and the displaced trigger track are explicitly excluded from the set of soft lepton candidates and from the set of tracks forming the jet candidates. The mass of the system formed by an eligible opposite-side track along with the trigger lepton and the displaced trigger track is required to be greater than about 5 $\mathrm{GeV/c^2}$. Soft lepton track candidates that belong to jets containing the trigger lepton are rejected, and so are track candidates for tagging jets which lie within a cone ΔR of 1.6 relative to the trigger lepton and displaced track system.

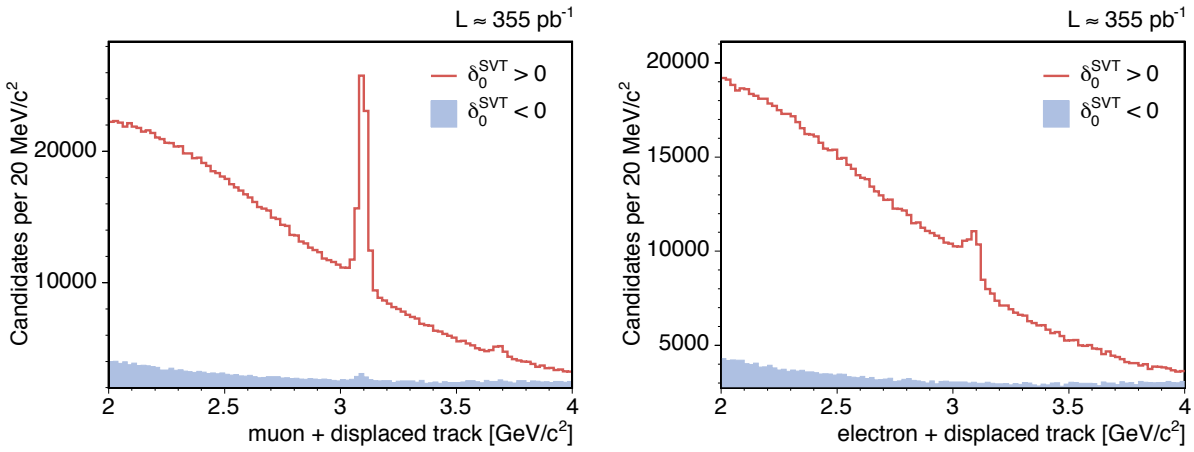

Figure 6.5: Mass distribution of the lepton and displaced track system, for the muon (left) and the electron (right) samples; the peaks at $\sim$ 3.1 GeV/c^2 correspond to $J/\psi \to l^+l^-$ decays.

Trigger side dilution correction

The OST dilution is calculated from the asymmetry in the number of events belonging to the classes of agreeing and disagreeing charges, between the trigger lepton and the opposite-side lepton or jet. The observed asymmetry however is decreased, *i.e. diluted*, due to effects related not solely to the opposite-side but also to the trigger-side. Denoting the corresponding asymmetry contributions by $\mathcal{D}$ and $\mathcal{D}_{trig}$, and to the extent that these are uncorrelated, the observed asymmetry $\mathcal{D}_{raw}$ is given by their product. That is,

$$\mathcal{D} \;=\; \frac{\mathcal{D}_{raw}}{\mathcal{D}_{trig}}\,, \tag{6.9}$$

which implies that the OST dilution is greater than the measured, raw asymmetry.

The trigger B may have undergone flavor oscillation by the time it decayed; also, the trigger lepton may have been produced in a sequential $b \to c \to l$ transition. Such trigger-side dilution effects are evaluated from Monte Carlo samples of semileptonic B decays including detector and trigger simulations. The dilution correction [78] is given by

$$\mathcal{D}_{trig} \;=\; 0.641 \pm 0.002\ (stat.) \pm 0.024\ (syst.)\ .$$

The OST dilution $\mathcal{D}$ is obtained, following (6.9), from the measured raw asymmetry and the above trigger-side correction.

Tagging power

We finally present the tagging performance of the opposite-side algorithms which have been described, as measured in the lepton and displaced track trigger sample.

The tagging efficiency is given by the fraction of events for which an eligible opposite-side object – soft lepton or jet – is identified. For the dilution, however, the achieved parameterizations imply that each tagged event is to be assigned a specific value, depending on the event properties accounted for through the dependencies implemented in each algorithm. The expected dilution and efficiency in each bin, $\mathcal{D}_k$ and ϵ_k, considering the discretized dependences, are combined to form the partial tagging power in the bin, $\epsilon_k \cdot \mathcal{D}_k^2$. The overall tagging power and efficiency are given by the sum over all bins,

$$\begin{aligned} \epsilon\mathcal{D}^2 &= \sum_k \epsilon_k \cdot \mathcal{D}_k^2 \,, \\ \epsilon &= \sum_k \epsilon_k \,. \end{aligned}$$

An *effective dilution* $\mathcal{D}_{\text{eff}}$ may then be defined as

$$\mathcal{D}_{\text{eff}} = \sqrt{\frac{\epsilon\mathcal{D}^2}{\epsilon}} \,.$$

The efficiency, effective dilution and tagging power for the soft lepton and jet charge taggers are summarized in Tables 6.1 and 6.2. The tagging performance is evaluated for the various algorithms separately. When applied to a given sample a fraction of events will be multiply tagged. For this reason, it also follows that the combined tagging power does not correspond simply to the sum of the partial $\epsilon\mathcal{D}^2$ contributions from the different algorithms.

soft lepton	ϵ [%]	$\mathcal{D}_{\text{eff}}$ [%]	$\epsilon\mathcal{D}^2$ [%]
muon, SMT	6.08 ± 0.04	33.9 ± 1.0	0.698 ± 0.042
electron, SET	14.22 ± 0.06	16.0 ± 0.7	0.366 ± 0.031

Table 6.1: Soft lepton tagging performance, for muon and electron algorithms.

6.2 Same side tagging

Same side tagging exploits the flavor-charge correlation between the B meson and associated particles produced nearby in phase space [79]. For each B meson species, the B and $\bar{B}$ states are expected to be more likely accompanied by leading fragmentation tracks of distinct charges. This is illustrated in Figure 6.6.

jet type	ϵ [%]	$\mathcal{D}_{\text{eff}}$ [%]	$\epsilon\mathcal{D}^2$ [%]
class 1, JVX	10.53 ± 0.03	18.9 ± 0.3	0.376 ± 0.011
class 2, JJP	28.52 ± 0.05	11.9 ± 0.2	0.404 ± 0.014
class 3, JPT	56.56 ± 0.07	5.0 ± 0.2	0.140 ± 0.011

Table 6.2: Jet charge tagging performance, for the three exclusive jet categories.

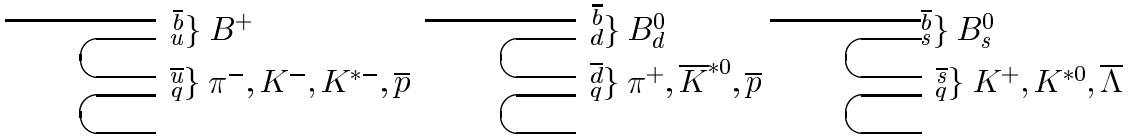

Figure 6.6: Charge correlation of B mesons with leading fragmentation tracks.

One can think of the hadronization process, in a simplified manner, as pulling light quark pairs from the vacuum and forming hadrons from nearby quarks. Consider for instance the case of a $B^0(\bar{b}d)$ meson. In order for it to be formed, the light quark pair which is nearest in the fragmentation chain to the initial heavy quark $\bar{b}$ must have been a $d\bar{d}$ pair. This leaves a $\bar{d}$ quark at the dangling end of the fragmentation chain. If the second nearest light quark pair is $u\bar{u}$, then the nearest meson in the fragmentation chain will be a π^+, which can be used to tag the flavor of the initial $\bar{b}$. If the second nearest light quark pair is a $d\bar{d}$ pair, then the nearest meson is a π^0, a neutral particle that therefore has no tagging power. However, the dangling end of the fragmentation chain remains a $\bar{d}$. If the third nearest light quark pair is a $u\bar{u}$ pair, then the second nearest meson will be a π^+, which can be used as a flavor tag.

Identical phenomenological descriptions as just offered for the B^0 mesons naturally hold for the other B meson species as well, the B^+ and the B_s. However the various possible hadrons which may be produced in the hadronization process associated to each B meson species lead to different overall likelihoods that a specific track charge is produced.

Additionally, also as pointed out in [79] the decay products of orbitally-excited B mesons usually referred to as B^{**} induce flavor-charge correlations which are coincident with those arising from fragmentation. Such B^{**} states correspond to P-wave levels of a b quark and a light antiquark, which may decay to $B\pi$. For instance, a B^{**+} can decay to $B^0\pi^+$ and not to $\bar{B}^0\pi^+$. These contributions are larger for B^+ than for B^0, and absent in the case of B_s mesons.

In summary, therefore, the following correlations are expected, on a statistical basis, between the production B meson flavor and a leading charged track:

- $B^+, \bar{B}^0, \bar{B}_s$ are more likely accompanied by a *negatively* charged track,

- B^-, B^0, B_s are more likely accompanied by a *positively* charged track.

The task of a SST algorithm is to identify such leading track in the event.

The same high statistics inclusive sample of a lepton and displaced track which was used to establish the OST methods in Section 6.1.3 cannot be used in the case of the SST method as its performance is expected not to be common for distinct B meson species. Instead, samples of fully reconstructed B decays will be employed to establish the algorithm performance from observed flavor asymmetries. These will be appropriate for the B^+ and B^0 mesons. The performance in the B_s case cannot however be extracted directly from corresponding data samples, and its evaluation is not addressed in the current chapter, being postponed until Chapter 9.

6.2.1 Algorithm

Candidate tracks are selected within an isolation cone of $\Delta R = 0.7$ relative to the B candidate. Tracks outside this region are used by the OST methods. The tags are expected to originate from the primary vertex, and the track candidates should thus be consistent with it: the z_0 is required to be within 2 cm, and the impact parameter d_0 is required to be within 10 standard deviations from zero. A minimum transverse momentum p_T of 450 MeV is imposed to avoid significant effects from charge asymmetries inherent to the detector performance for low momentum tracks.

Once the above selection criteria are imposed, there may be none, single or multiple tracks which are selected. The fraction of events for which the former occurs determines the efficiency. In case a single track is selected it becomes the tagging track. Otherwise, if there are multiple tag candidates, distinct track properties may be explored (as studied in Chapter 9) to select the tagging track. In the present algorithm implementation, the chosen track is that with the smallest momentum transverse to the direction given by the combined B and track momenta, p_T^{rel}, as indicated in Figure 6.7. String fragmentation models indicate that particles produced in the b quark hadronization chain have small momenta transverse to the direction of the b quark momentum.

6.2.2 Flavor asymmetry analysis

The evaluation of the SST algorithm performance is achieved in samples of fully reconstructed B decays, corresponding to an integrated luminosity of about 270 pb^{-1}. Decays of charged and neutral B mesons are used. The dilution for the B^+ mesons is obtained from the overall flavor asymmetry, while for the B^0 mesons a time dependent asymmetry analysis is implemented.

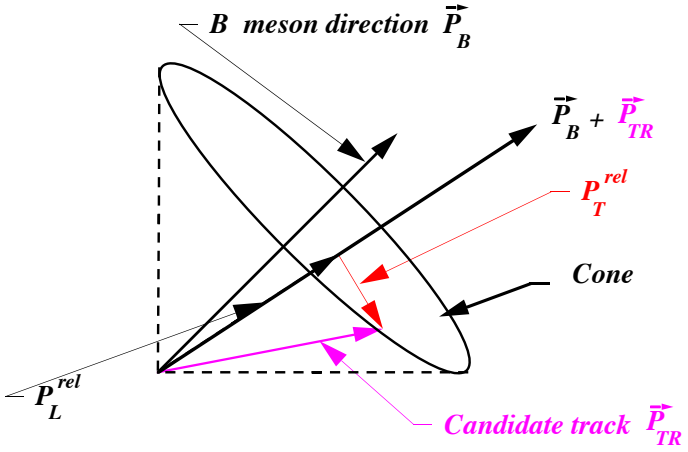

Figure 6.7: Illustration of the construction of the quantity p_T^{rel}.

Data samples

The charged and neutral B mesons are reconstructed in the following decay modes:

- $B^+ \to J/\psi K^+$, $B^+ \to \bar{D}^0\pi^+$,
- $B^0 \to J/\psi K^{*0}$, $B^0 \to D^{(*)-}\pi^+(\pi^+\pi^-)$.

The signal selection follows the criteria described in Chapter 4. The samples composition and corresponding mass distributions are also addressed therein.

Asymmetry

In order to measure the flavor asymmetries, each data sample is subdivided into three disjoint subsamples according to flavor tagging information. One such subsample contains the events for which no tagging track was found. The other two of these subsamples are obtained by comparing the charge of the selected tagging track with the B decay products, to determine whether or not the tagged production flavor coincides with the decay flavor. The mass distributions for each subsample are formed, and the obtained histograms are fitted to determine the corresponding number of signal events. Figure 6.8 shows the mass distributions for the flavor tagged B^+ candidates in the $J/\psi K$ subsamples.

In the case of charged B mesons, the measured numbers of signal events in each subsample are taken as estimates of the number of correctly tagged N_r, incorrectly tagged N_w, and non-tagged N_n events. These are in turn used to compute the efficiency (6.1) and the dilution (6.2) of the tagging method.

	ϵ [%]	$\mathcal{D}$ [%]	$\epsilon\mathcal{D}^2$ [%]
B^+	61.0 ± 0.5	19.5 ± 1.4	2.33 ± 0.34
B^0	63.7 ± 0.9	12.8 ± 2.2	1.00 ± 0.35

Table 6.3: Same side tagging algorithm performance for B^+ and B^0 mesons.

For samples of neutral B mesons, the measured flavor asymmetry corresponds not only to the tagging dilution but contains also the effects of flavor mixing. The strategy in this case is to measure the asymmetry as above, but in given ranges of proper decay time t. Finally the asymmetry dependency on proper time is fitted with the model

$$A(t_i) \;=\; \frac{\{e^{-t_i/\tau}\,\mathcal{D}\,\cos(\Delta m_d\, t_i)\} \otimes G(t_i;\sigma_t)}{e^{-t_i/\tau} \otimes G(t_i;\sigma_t)\;.} \tag{6.10}$$

where τ and Δm_d stand for the lifetime and oscillation frequency of the B^0 system, and σ_t is the proper decay time resolution; t_i denotes the mean value of the respective proper decay time bin. The measured asymmetries for each proper time bin are illustrated in Figure 6.9 for the $B^0 \to D^-\pi^+$ decay sample, along with the fitted time-dependent asymmetry (6.10) projection.

The combined results for the SST algorithm performance obtained from fits of the charged and neutral B meson samples are summarized in Table 6.3.

The value of the oscillation frequency of the B^0 system, which appears in (6.10), is simultaneously extracted. From the combined fit of the studied neutral modes we obtain

$$\Delta m_d = 0.526 \pm 0.056\ (\text{stat.}) \pm 0.005\ (\text{syst.})\ \text{ps}^{-1}\;.$$

The quoted systematic uncertainty was evaluated by varying the range and parameters in the individual mass fits, the effect of swapped candidates in $J/\psi K^*$, as well as the proper time resolution (varied from 0 to 90 μm), which provide the leading contributions. This constitutes the first mixing measurement performed at Run II. It is also the first time such a measurement is performed at a hadron collider using fully reconstructed decays.

6.3 Combination of flavor taggers

The same-side and opposite-side tagging algorithms provide complementary information on the B mesons production flavor. This information must be combined as input to the mixing analysis for achieving optimal sensitivity. Two general approaches may be considered: sequential application of independent algorithms, and algorithm merging employing multivariate methods. At the beginning we adopt the former, which has the advantage of offering

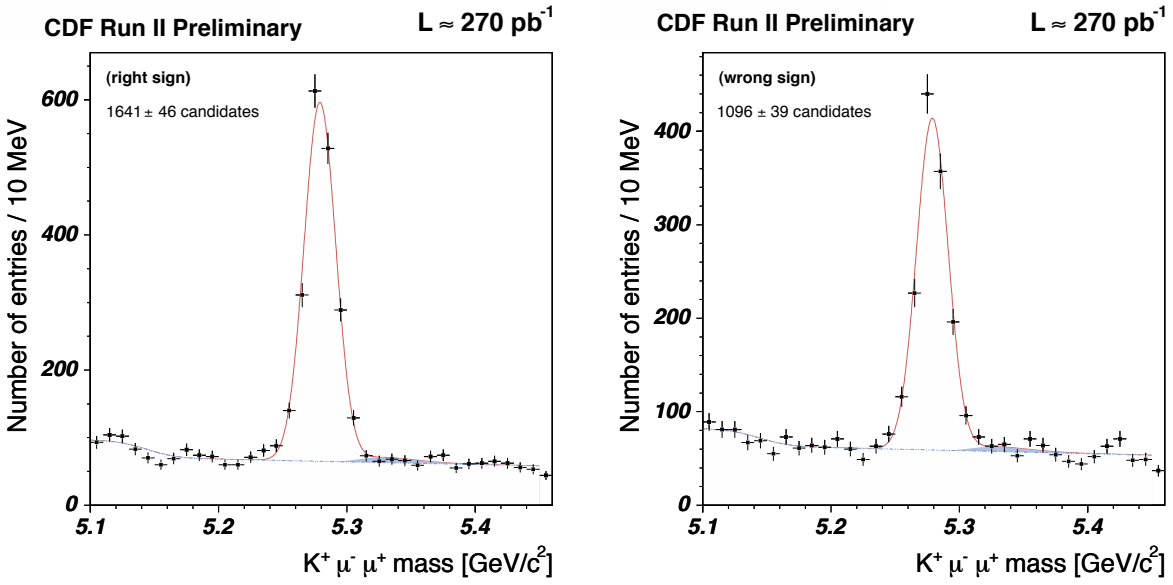

Figure 6.8: Mass distributions of $B^+ \to J/\psi K^+$ SST-tagged candidates, for which the charges of the kaon and the tagging track disagree (left) and agree (right); the signal yields in the two samples are used to determine the tagging dilution.

best insight and control of individual contributions. Ultimately however the latter option will be also explored as part of a final analysis optimization.

6.3.1 Dilution factors

Measurements are in general affected by various experimental effects, stemming, for instance, from detector characteristics and resolutions, and sample backgrounds. In mixing analyses, the performance of the flavor tagging methods plays additionally a prominent role. These sources effectively translate into dilution factors, which dampen the observable amplitude of the oscillations and decrease the sensitivity of the sample. In Section 11.1 we have described the contribution from various of these sources.

Flavor tagging deals with the determination of which state, B or $\bar{B}$, the meson is at a given stage. The tagging dilution $\mathcal{D}$ provides an estimate of the probability that such decision is correct. This probability for a flavor method α is given by $p_\alpha = \frac{1+\mathcal{D}_\alpha}{2}$, while the mistagging probability is the complement to unity, $1 - p_\alpha$.

In general the determination of the B flavor needs to be performed in different circumstances, employing distinct tagging approaches. For example, a comparison of the flavor at production and decay times is necessary to infer the mixed or unmixed classification of the

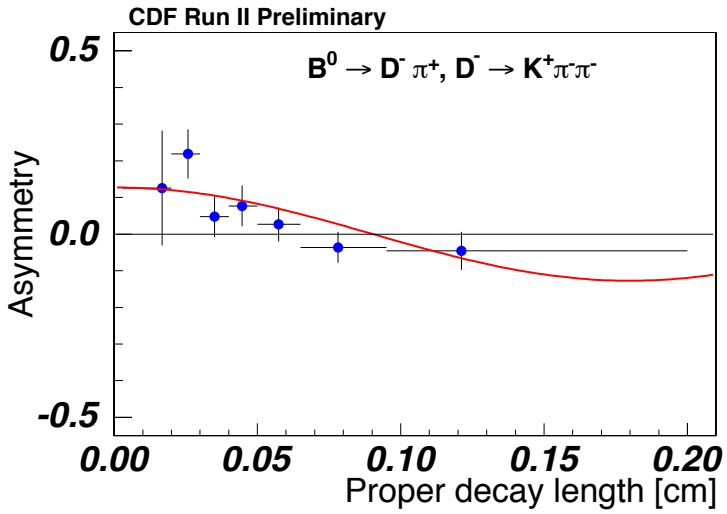

Figure 6.9: Time-dependent flavor asymmetry for $B^0 \to D^-\pi^+$ candidates tagged by the SST algorithm; the oscillation pattern is determined by the mixing frequency Δm_d and the corresponding amplitude is given by the tagging dilution.

event. The flavor of the meson at decay time may be obtained from its decay products, when flavor specific decays are employed. This determination becomes more unambiguous the more accurate and complete the reconstruction of the decay chain is. When the candidate reconstruction is pursued in a more inclusive fashion, more elaborate techniques may be used and their respective dilutions estimated.

We are considering systems characterized by two possible states or outcomes. That is, the meson is determined to be in either a particle or antiparticle state. Mixing is itself a two-state physics process: the meson, once detected, is either in the same or the opposite flavor state than when it was produced. In the latter case the associated dilution is given by the cosine term. For such systems it may be useful to define the matrix

$$O(\mathcal{D}_\alpha) \;=\; \begin{bmatrix} p_\alpha & 1-p_\alpha \\ 1-p_\alpha & p_\alpha \end{bmatrix} = \begin{bmatrix} \frac{1+\mathcal{D}_\alpha}{2} & \frac{1-\mathcal{D}_\alpha}{2} \\ \frac{1-\mathcal{D}_\alpha}{2} & \frac{1+\mathcal{D}_\alpha}{2} \end{bmatrix} ,$$

with

$$\mathcal{D}_\alpha = |O(\alpha)| = 2p_\alpha - 1 \; .$$

When two separate systems are involved, one may write

$$O(\mathcal{D}_\alpha) \cdot O(\mathcal{D}_\beta) \;=\; O(\mathcal{D}_\alpha \cdot \mathcal{D}_\beta) \; .$$

That is, the dilution factors multiply together.

When multiple tagging methods are employed to determine the flavor of the meson at a common stage, the flavor information may be combined, an issue which we address below.

6.3.2 Independent taggers

This section deals with the proper decay time likelihood description for events tagged by independent algorithms. The combination of flavor information obtained from multiple tagging algorithms has been addressed elsewhere [98].

Consider independent taggers $\{T_i\}$, each characterized by efficiency ϵ_i and dilution D_i. Denote the probability of decision by tagger T_i to be correct as $p_i^{rs} = \frac{1+D_i}{2}$ and incorrect as $p_i^{ws} = \frac{1-D_i}{2}$. The probability that the B meson has not mixed is $p_{um} = \frac{1+\cos(wt)}{2}$, and that it did mix is $p_m = \frac{1-\cos(wt)}{2}$. For neutral mesons, $w = \Delta m$ is the mixing frequency, while for charged mesons, $w = 0$. Let $p_i^{\pm}$ denote the probability for tagger T_i to give observable tagging decision $\pm$; here, the decision being"'+" ("-") denotes that the production and decay flavors coincide (are opposite).

For the case of a single tagger, T_i, the probability for an event in the sample to be tagged is ϵ_i, and for it not to be tagged is $1 - \epsilon_i$. For the case of two taggers, T_i and T_j, the probability for an event to be tagged by both algorithms is $\epsilon_i \cdot \epsilon_j$, for it to be tagged by T_i alone is $\epsilon_i \cdot (1 - \epsilon_j)$, and by none of the algorithms is $(1 - \epsilon_i) \cdot (1 - \epsilon_j)$. Schematically,

$$p_\epsilon(\xi) = \begin{cases} (1-\epsilon_1)(1-\epsilon_2) & (\xi_1 = 0,\ \xi_2 = 0) \\ \epsilon_1(1-\epsilon_2) & (\xi_1 = \pm 1,\ \xi_2 = 0) \\ (1-\epsilon_1)\epsilon_2 & (\xi_1 = 0,\ \xi_2 = \pm 1) \\ \epsilon_1\epsilon_2 & (\xi_1 = \pm 1,\ \xi_2 = \pm 1) \end{cases} .$$

Assuming now that the event is tagged by a single algorithm, we are interested in expressing the probability for observing a particular decision. For example, a "+" decision can be arrived at in case the meson did not mix and the tagger gave the correct answer, or if an incorrect answer was given for a meson which did mix. This is expressed simply as follows,

$$\begin{aligned} p_i^+ &= p_i^{rs} \cdot p_{umix} + p_i^{ws} \cdot p_{mix} \\ &= \frac{1+D_i}{2} \cdot \frac{1+\cos(wt)}{2} + \frac{1-D_i}{2} \cdot \frac{1-\cos(wt)}{2} \\ &= \frac{1+D_i \cdot \cos(wt)}{2} . \end{aligned}$$

More generally, the probability for a non-trivial decision ξ is expressed as

$$p_i^\xi = \frac{1}{2}[1 + \xi D_i \cdot \cos(wt)] \qquad (\mathrm{singly-tagged}).$$

Next we extend this reasoning to find the corresponding expressions for events simultaneously tagged by independent algorithms. For example, we would like to evaluate the probability p^{++} that both taggers, T_1 and T_2, give "+" decisions. Despite the algorithms

being independent, the equality $p^{++} = p_1^+ \cdot p_2^+$ does not in general hold; this is so due to physics-level correlations, *i.e.* mixing. Instead, and analogously to the single tagger case above, a positive decision for both taggers may be arrived at in case the meson did not mix and the taggers gave the correct answer, or if an incorrect answer was given and the meson did mix. This is expressed as follows,

$$\begin{aligned} p^{++} &= p_1^{rs} \cdot p_2^{rs} \cdot p_{um} + p_1^{ws} \cdot p_2^{ws} \cdot p_m \\ &= \frac{(1 + D_1 D_2) + (D_1 + D_2) \cdot \cos(wt)}{4} \, . \end{aligned}$$

More generally, the probability for non-trivial decisions ξ_1 and ξ_2 is expressed as

$$p^{\xi_1 \xi_2} = \frac{1}{4}[(1 + \xi_1 \xi_2 D_1 D_2) + (\xi_1 D_1 + \xi_2 D_2) \cdot \cos(wt)] \qquad (\text{doubly} - \text{tagged}) \, .$$

The treatment of the possible combinations of tagging decisions is specified in Table 6.4. A general expression can be formally written as

$$P(\xi|t) = \frac{(1 + \xi_1 \xi_2 D_1 D_2) + (\xi_1 D_1 + \xi_2 D_2) \cos(wt)}{(1 + |\xi_1|)(1 + |\xi_2|)} \, .$$

ξ_1	ξ_2	efficiency factors	tagging decision probabilities	
0	0	$(1-\epsilon_1)\cdot(1-\epsilon_2)$	1	1
+	0	$\epsilon_1 \cdot(1-\epsilon_2)$	$p_1^{rs} \cdot p_{um} + p_1^{ws} \cdot p_m$	$\frac{1+D_1\cdot\cos(wt)}{2}$
-	0	$\epsilon_1 \cdot(1-\epsilon_2)$	$p_1^{rs} \cdot p_m + p_1^{ws} \cdot p_{um}$	$\frac{1-D_1\cdot\cos(wt)}{2}$
0	+	$(1-\epsilon_1)\cdot \epsilon_2$	$p_2^{rs} \cdot p_{um} + p_2^{ws} \cdot p_m$	$\frac{1+D_2\cdot\cos(wt)}{2}$
0	-	$(1-\epsilon_1)\cdot \epsilon_2$	$p_2^{rs} \cdot p_m + p_2^{ws} \cdot p_{um}$	$\frac{1-D_2\cdot\cos(wt)}{2}$
+	+	$\epsilon_1 \cdot \epsilon_2$	$p_1^{rs} \cdot p_2^{rs} \cdot p_{um} + p_1^{ws} \cdot p_2^{ws} \cdot p_m$	$\frac{(1+D_1D_2)+(D_1+D_2)\cdot\cos(wt)}{4}$
-	-	$\epsilon_1 \cdot \epsilon_2$	$p_1^{rs} \cdot p_2^{rs} \cdot p_m + p_1^{ws} \cdot p_2^{ws} \cdot p_{um}$	$\frac{(1+D_1D_2)-(D_1+D_2)\cdot\cos(wt)}{4}$
+	-	$\epsilon_1 \cdot \epsilon_2$	$p_1^{rs} \cdot p_2^{ws} \cdot p_{um} + p_1^{ws} \cdot p_2^{rs} \cdot p_m$	$\frac{(1-D_1D_2)+(D_1-D_2)\cdot\cos(wt)}{4}$
-	+	$\epsilon_1 \cdot \epsilon_2$	$p_1^{rs} \cdot p_2^{ws} \cdot p_m + p_1^{ws} \cdot p_2^{rs} \cdot p_{um}$	$\frac{(1-D_1D_2)+(D_2-D_1)\cdot\cos(wt)}{4}$

Table 6.4: Probability factors for the possible decisions of two independent taggers.

Same side tagging in inclusive modes

In partially reconstructed modes, the tag-track chosen by the SST algorithm may belong to the B decay products. Indeed, in $B \to DlX$ modes, in a fraction (f_{**}) of the times a decay track, denoted π^{**}, is selected as the tag-track; this notation will be used in the following. Also, the first (second) tagger will be identified with the same (opposite) side algorithm: $T_1 = SST$ and $T_2 = OST$.

The charge of the lepton and that of the π^{**} are anti-correlated (Tables 4.17 and 4.18). As both the lepton and the π^{**} are final-state tracks, no information of the B initial flavor can be inferred, when the π^{**} is selected by the algorithm. Accordingly, the overall probability for a SST decision is given by

$$\begin{aligned} p_1^+ &= (1-f_{**})\cdot\frac{1+D_1\cdot\cos(wkt)}{2} \\ p_1^- &= (1-f_{**})\cdot\frac{1-D_1\cdot\cos(wkt)}{2}+f_{**} \end{aligned}$$

This may be summarized as

$$P(\xi|t) = (1-f_{**})\cdot\frac{1+\xi D_1\cdot\cos(w\kappa t)}{(1+|\xi|)}+f_{**}\cdot\frac{1-\xi}{2}|\xi| \ .$$

Here κ denotes the kinematical correction factor (5.8) required by the partial proper time reconstruction.

For studying the case when an event is tagged simultaneously by SST and OST, it is useful to consider first the hypotheses that a π^{**} is and is not selected by the SST. For the sake of concreteness, consider the evaluation of the case the SST yields decision "-" and the OST gives decision "+".

In the hypothesis that a π^{**} is not selected by the SST, the probability for the decisions is correlated to that of the B to have mixed. It is expressed as

$$\begin{aligned} p^{-+} &= p_1^{ws}\cdot p_2^{rs}\cdot p_{um}+p_1^{rs}\cdot p_2^{ws}\cdot p_m \\ &= \frac{(1-D_1D_2)+(D_2-D_1)\cdot\cos(wkt)}{4} \end{aligned}$$

In the hypothesis that a π^{**} is selected by the SST, no physics-level correlations need to be considered (as the π^{**} does not carry initial flavor information), and the probability can be expressed as

$$p^{-+} = p_1^-\cdot p_2^+ = 1\cdot\frac{1+D_2\cdot\cos(wkt)}{2}$$

The possible combinations of other non-trivial decisions can be evaluated in a similar fashion, and the result may be represented as

$$\begin{aligned} p^{\xi_1\xi_2} &= (1-f_{**})\cdot\frac{1}{4}[(1+\xi_1\xi_2D_1D_2)+(\xi_1D_1+\xi_2D_2)\cdot\cos(wkt)] \\ &+ \quad f_{**}\cdot\frac{1-\xi_1}{2}\cdot\frac{1+\xi_2D_2\cdot\cos(wkt)}{2} \ . \end{aligned}$$

The general expression summarizing the possible tagging decision combinations is accordingly written as

$$\begin{aligned} P(\xi|t) &= (1-f_{**})\cdot\frac{(1+\xi_1\xi_2D_1D_2)+(\xi_1D_1+\xi_2D_2)\cdot\cos(wkt)}{(1+|\xi_1|)(1+|\xi_2|)} \\ &+ \quad f_{**}\cdot\frac{1-\xi_1}{2}|\xi_1|\cdot\frac{1+\xi_2D_2\cdot\cos(wkt)}{1+|\xi_2|} \ . \end{aligned}$$

sam

6.4 Résumé

The determination of the b flavor at production time is a crucial task in the study of flavor oscillations. It is accomplished by the so-called flavor tagging methods which have been presented, and which will be employed in the following chapters.

B mesons are produced from the hadronization of b and $\bar{b}$ quarks which are originally produced in $b\bar{b}$ pairs. The determination of whether a B meson resulted from the hadronization of a b or a $\bar{b}$ quark can accordingly be achieved in two fashions. It can be inferred from information carried by tracks in the vicinity of the B candidate, or by the fragmentation or decay products of the other, accompanying b-hadron in the event. The corresponding classes of flavor tagging algorithms are called *same side* and *opposite side* methods, respectively, and denoted in short by SST and OST.

The aim of the SST is to detect the production flavor of the trigger B meson by identifying the leading accompanying fragmentation track. The objective of the OST is to tag the flavor of the b-hadron that did not fire the trigger to determine the flavor of the trigger B meson when it was produced. Two distinct OST strategies are explored. One, called soft lepton tagger, aims at identifying the leptons which originate from semileptonic decays of the opposite-side b-hadron. The other OST method, called jet charge tagger, explores the charges of the tracks surrounding the b-hadron direction whose combination is correlated to the charge of the b-quark itself.

The tagging power of an algorithm is given by $\epsilon\mathcal{D}^2$, where the efficiency ϵ corresponds to the fraction of events which are tagged, and the dilution $\mathcal{D}$ is related to the probability for the algorithm to provide a correct flavor determination. The OSTs are established in an inclusive sample of semileptonic decays. The high statistics of this sample further allows for the algorithms' performance to be parameterized which translates into increased power. The performance of the SST is dependent on the species of B meson candidates being tagged. The algorithm is thus preferably established in samples of fully reconstructed B meson decays. The tagging performance is summarized as:

method	tagging power, $\epsilon\mathcal{D}^2$ [%]
opposite-side (sum)	1.98 ± 0.26
same-side, B^+	2.33 ± 0.34
same-side, B^0	1.00 ± 0.35

When applied to samples of B^0 decays, a preliminary measurement of the oscillation frequency Δm_d is achieved, establishing the feasibility of mixing analyses at CDF II. The SST performance for B_s mesons cannot be extracted directly from data, before a signal is firmly established. This matter will be further addressed in Chapter 9. The issue of exploring the tagging information from different algorithms has been addressed, and the technique also employed in ensuing chapters.